

# Studies on targets for inertial fusion ignition demonstration at the HiPER facility

S. Atzeni<sup>1</sup>, J.R. Davies<sup>2</sup>, L. Hallo<sup>3</sup>, J.J. Honrubia<sup>4</sup>, P.H. Maire<sup>3</sup>,  
M. Olazabal-Loume<sup>3</sup>, J.L. Feugeas<sup>3</sup>, X. Ribeyre<sup>3</sup>, A. Schiavi<sup>1</sup>,  
G. Schurtz<sup>3</sup>, J. Breil<sup>3</sup> and Ph. Nicolai<sup>3</sup>

<sup>1</sup> Dipartimento di Energetica, Università di Roma 'La Sapienza' and CNISM,  
Via A. Scarpa, 14, 00161 Roma, Italy

<sup>2</sup> GolP, Instituto de Plasma e Fusão Nuclear, Instituto Superior Tecnico, 1049-001 Lisbon,  
Portugal

<sup>3</sup> CELIA, Université Bordeaux 1, Talence, France

<sup>4</sup> E.T.S.I. Aeronáuticos, Universidad Politécnica de Madrid, Spain

E-mail: [stefano.atzeni@uniroma1.it](mailto:stefano.atzeni@uniroma1.it)

Received 22 December 2008, accepted for publication 18 March 2009

Published 9 April 2009

Online at [stacks.iop.org/NF/49/055008](http://stacks.iop.org/NF/49/055008)

## Abstract

Recently, a European collaboration has proposed the High Power Laser Energy Research (HiPER) facility, with the primary goal of demonstrating laser driven inertial fusion fast ignition. HiPER is expected to provide 250 kJ in multiple,  $3\omega$  (wavelength  $\lambda = 0.35 \mu\text{m}$ ), nanosecond beams for compression and 70 kJ in 10–20 ps,  $2\omega$  beams for ignition. The baseline approach is fast ignition by laser-accelerated fast electrons; cones are considered as a means to maximize ignition laser–fuel coupling. Earlier studies led to the identification of an all-DT shell, with a total mass of about 0.6 mg as a reference target concept. The HiPER main pulse can compress the fuel to a peak density above  $500 \text{ g cm}^{-3}$  and an areal density  $\rho R$  of about  $1.5 \text{ g cm}^{-2}$ . Ignition of the compressed fuel requires that relativistic electrons deposit about 20 kJ in a volume of radius of about  $15 \mu\text{m}$  and a depth of less than  $1.2 \text{ g cm}^{-2}$ . The ignited target releases about 13 MJ. In this paper, additional analyses of this target are reported. An optimal irradiation pattern has been identified. The effects on fuel compression of the low-mode irradiation non-uniformities have been studied by 2D simulations and an analytical model. The scaling of the electron beam energy required for ignition (versus electron kinetic energy) has been determined by 2D fluid simulations including a 3D Monte Carlo treatment of relativistic electrons, and agrees with a simple model. Integrated simulations show that beam-induced magnetic fields can reduce beam divergence. As an alternative scheme, shock ignition is studied. 2D simulations have addressed optimization of shock timing and absorbed power, means to increase laser absorption efficiency and the interaction of the igniting shocks with a deformed fuel shell.

**PACS numbers:** 52.57.–z, 52.57.Kk, 52.40.Mj

(Some figures in this article are in colour only in the electronic version)

## 1. Introduction

High Power Laser for Energy Research (HiPER) is a proposed facility aiming at the demonstration of the feasibility of fast ignition [1, 2]. We recall that fast ignition [3, 4] is an approach to inertial confinement fusion in which the stages of fuel compression and ignition are separated. The fuel is first compressed to high density by a suitable driver; the precompressed fuel is ignited by a second ultraintense driver. To achieve its goal HiPER will deliver a  $3\omega$  multi-beam

pulse of about 250 kJ in about 10 ns, and a  $2\omega$  or  $3\omega$  ignition pulse of about 70 kJ in 15–20 ps. (Here  $\omega$  refers to the fundamental frequency of the Nd:glass laser, with a wavelength of  $1.053 \mu\text{m}$ .) The baseline approach is fast ignition by laser-accelerated fast electrons; cones [5, 6] are being considered as a means to maximize ignition laser–fuel coupling. A reference fusion capsule concept for HiPER was identified by previous studies [2, 7, 8]. Capsule and laser pulse were then designed on the basis of one-dimensional (1D) simulations of irradiation and implosion. Care was taken to

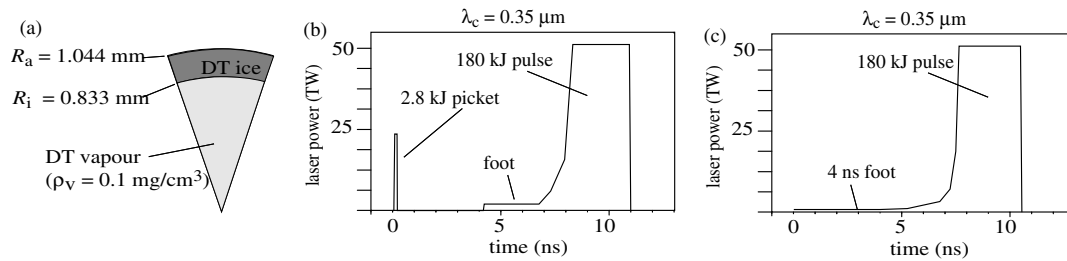


Figure 1. Reference capsule and laser pulses.

limit both plasma and hydrodynamic (Rayleigh–Taylor, RTI) instabilities. Two-dimensional (2D) simulations of the final implosion stage and ignition of cone-in-shell capsules have been carried out and presented elsewhere (see section 3 of [8]). Nevertheless, the issues related to the interaction of a guiding cone and the imploding fuel [9] are not addressed here. Ignition of the precompressed fuel by electron beams was studied by 2D simulations. Sensitivity to pulse shaping [10] and to variation of some of the igniting beam parameters was also addressed [2, 7, 8]. A key issue for the feasibility of the scheme is the efficient transfer of the energy of the ignition laser beam to the hot spot, which involves laser absorption, fast electron generation, fast electron transport and energy deposition and the effect of the cone on both fuel compression and beam coupling. Another important aspect concerns the realistic description of the laser irradiation scheme, and the consequences of the unavoidable irradiation non-uniformities.

In Spring 2008 the HiPER project entered a three-year preparatory phase, with the goal of achieving a detailed design. In this paper, after a brief description of the present reference capsule concept (section 2), we present the first results of this effort. We discuss the design of the irradiation scheme for fuel compression, and study the effect of low-mode irradiation non-uniformities on the fuel assembly of spherical targets (section 3). We then present studies of the ignition stage based on improved 3D models of electron transport in the compressed fuel and more realistic models of the electron beams (section 4). In section 5, we present results on shock ignition [11] of the HiPER reference capsule. We consider this concept because, similarly to fast ignition, it separates the stages of compression and ignition and employs an intense (but not ultraintense) pulse for ignition. However, it appears potentially attractive since it does not rely on the generation and transport of relativistic electrons. Some conclusions are drawn in section 6.

## 2. Target concept

The target concept under investigation is a simple shell, with an inserted cone. A preliminary reference shell has been identified as a result of the study summarized in [7, 8]. This is an all-DT shell, with a total mass of 0.58 mg and the dimensions indicated in figure 1(a). The shell and target parameters have been chosen to satisfy a number of constraints, including the following: (i) the fuel has to be compressed to average density in excess of  $300 \text{ g cm}^{-3}$ , with a confinement parameter  $\rho R \simeq 1.5 \text{ g cm}^{-2}$ ; (ii) the fuel average entropy should be kept as small as possible (i.e. the insentropie parameter should be about 1); (iii) the intensity of the compression pulse should

be smaller than  $5 \times 10^{14} \text{ W cm}^{-2}$  (at  $3\omega$ ) to limit plasma instabilities; (iv) the RTI exponential growth factor should be limited to 6–7 for the fastest growing mode (using the criterion suggested in [12]); (v) the in-flight-aspect ratio should be limited to 30–35. The requests on plasma instabilities and RTI led to the choice of a moderately thin target (a thicker target, such as that studied in [13] requires higher intensity) and of the pulse shape. Indeed, the reference laser compression pulse, shown in figure 1(b), consists of a short intense picket, preceding a low intensity foot, a properly tailored rise and a main pulse. The initial picket preceding the main pulse serves to implement adiabat shaping [14]. This allows one to increase the entropy of the ablator (to reduce RTI growth), while at the same time keeping the entropy of the inner fuel at a very low level. Irradiation, implosion and compression of the capsule have been studied by three different 1D codes, which produce results in substantial agreement [8, 10, 15]. According to the most accurate and realistic simulations, the target achieves a peak density higher than  $600 \text{ g cm}^{-3}$  and  $\rho R \simeq 1.5 \text{ g cm}^{-2}$ , when driven by a pulse of about 180 kJ (absorbed with an efficiency of 67%). Half of the initial mass is imploded, at a (peak) velocity of  $2.8 \times 10^7 \text{ cm s}^{-1}$ . In addition to the reference pulse, we have also considered a pulse without initial picket (see figure 1(c)), leading to essentially identical performances. This is more susceptible to RTI, but studies with a perturbation code [10] led to more optimistic results than the simple model used in [7], and indicated that RTI growth could still be acceptable. Detailed simulations are then required to resolve this issue, and are planned for the near future.

Ignition of the compressed fuel occurs if about 20 kJ are deposited in 15 ps in a cylindrical volume with a radius of  $15 \mu\text{m}$  and a mass depth of  $1\text{--}1.2 \text{ g cm}^{-2}$ ; the ignited target releases about 13 MJ of fusion energy. Actual beams reaching the dense fuel have to deliver larger energy to account for inefficiencies due to electron scattering and broad energy distribution of the electrons. The average kinetic energy (temperature) of such electron beams should be 1–1.5 MeV [8]. The crucial issue for the design of the HiPER target then seems to be the coupling efficiency of the ultraintense beam, which must exceed 20%. This implies good conversion of the laser energy into a forward collimated beam of hot electrons with the desired temperature. Using a standard ponderomotive scaling for the average energy of the hot electrons [16],  $\bar{\epsilon} \text{ (MeV)} = [I_{\text{laser}} / (1.3 \times 10^{19} \text{ W cm}^{-2})]^{1/2} \cdot \lambda \text{ (}\mu\text{m)}$ , such conditions could be met by a laser pulse with an intensity somewhat in excess of  $10^{20} \text{ W cm}^{-2}$ , and  $2\omega$  or  $3\omega$  frequency (lower frequencies resulting in the generation of too much energetic electrons). We note, however, that recent studies [17] show that the hot

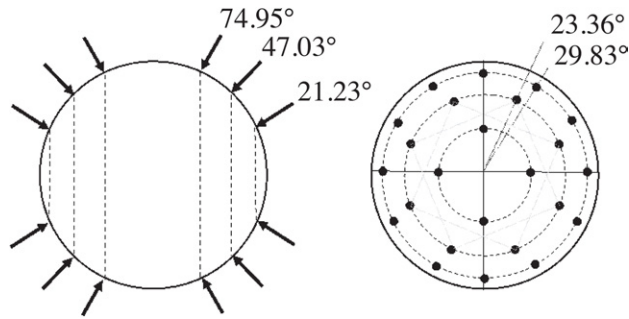


**Figure 2.** The 48 beams HiPER illumination scheme.

electron temperature can be well below that predicted by the above scaling. This may allow for ignition pulses at the fundamental frequency  $\omega$ .

### 3. Fuel capsule irradiation and generation of the compressed fuel assembly

#### 3.1. Beam pattern and irradiation uniformity

The irradiation pattern for HiPER has been defined by using the geometrical optics code CECLAD. We choose a 48 beams configuration pattern [18] made of 3 rings on each side of the target hemispheres ( $21.23^\circ$ ,  $47.03^\circ$ ,  $74.95^\circ$ ). The rings have, respectively, 4, 8 and 12 beams. The offsets are  $0^\circ$  for the 4 beams on the first ring,  $\pm 23.4^\circ$  for the 8 ( $4 + 4$ ) beams of the second ring and  $0^\circ$  and  $\pm 29.8^\circ$  for the 12 ( $4 + 4 + 4$ ) beams of the last ring (see figure 2). Each beam has a super gaussian distribution of intensity in the focal spot, in the form  $I(r) = \exp(-r/a)^{2m}$ . Parameters  $m$  and  $a$  are chosen such as to minimize the irradiation non-uniformity  $\sigma_{\text{rms}}$ . According to our computations a minimum  $\sigma_{\text{rms}} = 0.15\%$  is obtained for  $m = 1.02$  and  $a = 0.61 R_a$ , where  $R_a$  is the initial outer radius of the target (see figure 1). The implosion dynamics causes the critical radius to decrease in time; however, the symmetry indicator  $\sigma_{\text{rms}}$  remains stable during this whole process.

The robustness of this pattern with respect to random deviations from nominal was evaluated: the symmetry indicator  $\sigma_{\text{rms}}$  remains close to 1% under a normal repartition of the beam to beam imbalance (10%), of the beam pointing (5%), and of the beam centering (2% of initial target radius). In order to give input to low-mode asymmetry studies, a Legendre polynomial expansion has also been carried out. It shows that the main modes of illumination non-uniformity are  $l = 12$ , 8 and 10, with a maximum relative non-uniformity of 0.5% for mode  $l = 12$ .

#### 3.2. Fuel assembly under low-mode asymmetry

We have then studied the effect on capsule implosion of laser illumination non-uniformities [19]. We assume perfectly smooth focal spots, so the non-uniformity spectrum consists of low modes only. Typically modes  $1 < l < 20$  of a Legendre expansion of the incident laser intensity on the target surface are considered. The main part of our analysis relies on a linear model of the ablative Rayleigh–Taylor (ARTI) growth of the induced perturbation.

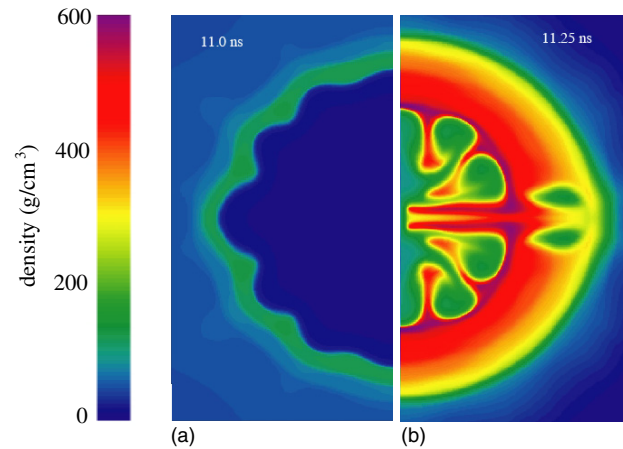


**Figure 3.** Multimode CHIC simulation of the HiPER reference target. 2D density maps: (a) at time  $t = 11.0$  ns; (b) at time  $t = 11.25$  ns. It is apparent that large deformations only occur during the stagnation phase.

The linear assumption is justified by 2D implosion simulations using the multimode irradiation spectrum provided by CECLAD [19]. It turns out that the  $l = 12$  mode dominates at all times and little mode coupling occurs; the amplitude of the perturbation of the compressed fuel remains moderate until somewhat before the time of maximum compression (see figure 3). We have then used an ARTI model employing established theory [20]. The input parameters of the model (acceleration, Froude number, thermal conductivity exponent, density gradient scale-length) are taken from 1D numerical CHIC [21] calculations.

Model results are shown to agree reasonably well with CHIC single-mode calculations at  $l = 12$ –20; at lower  $l$  the model predicts larger growth than 2D CHIC simulations [19]. The ARTI model has then been used to predict areal density modulations at stagnation time for different target designs and irradiation patterns. This allows to estimate effective areal densities and then expected target yields. For the irradiation pattern of figure 2, the ratio of the perturbed yield to the 1D yield is estimated to be 0.80 for the HiPER baseline target. However, the sensitivity of ignition to areal density perturbations at stagnation strongly depends on the considered ignition process, and can only be assessed by 2D ignition calculations. An example will be shown in section 5.3.

### 4. Electron beam driven ignition of the compressed fuel

Accurate determination of the ignition conditions is a key element of target design. Studies on the ignition of the HiPER reference capsule showed that the minimum ignition energy  $E_{\text{ig}}$  depends critically on the average electron energy  $\bar{E}$  and on beam divergence [8, 22, 23]. Here, we show that the dependence of  $E_{\text{ig}}$  on  $\bar{E}$  can be accurately reproduced by a simple model (section 4.1). In addition, we show that beam-induced magnetic fields can reduce beam divergence (section 4.2).

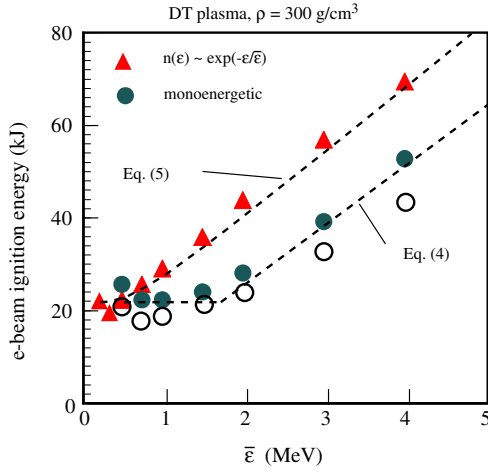


**Figure 4.** Ignition energy from full simulations (filled symbols) and approximated expressions (dashed curves). The void circles refer to simulations for monoenergetic beams, neglecting scattering.

#### 4.1. Minimum ignition energy: dependence on the electron kinetic energy

In [24] the minimum ignition energy of a uniform, equimolar DT sphere with density  $\rho$  was calculated using the 2D hydro-code DUED (see [25] and references therein) by assuming that a cylindrical region with depth  $\mathcal{P}$ , corresponding to the penetration depth, was heated by particles with constant stopping power, giving [24, 26]

$$E_{\text{ig}} = 18 \left( \frac{\rho}{300 \text{ g cm}^{-3}} \right)^{-1.85} \max \left( 1, \frac{\mathcal{P}}{1.2 \text{ g cm}^{-2}} \right) \text{ kJ.} \quad (1)$$

This is not directly applicable to electron fast ignition because non-uniform stopping power, angular scattering and the broad energy distribution of laser-generated electron beams lead to a wide range of penetration depths. To address this we have added a 3D Monte Carlo electron energy deposition routine to DUED; the expressions for the stopping power and the scattering coefficients are given in [27] (see also [28]). The first application of this improved model was to ignition of the HiPER capsule [8]. We now show how equation (1) can be modified to agree with the new model and to explicitly include the dependence on electron kinetic energy.

We have repeated the calculations from [24] for parallel, cylindrical electron beams with uniform intensity profiles, a constant power, a radius of  $20 \mu\text{m}$  and a pulse duration of  $20 \text{ ps}$  at  $\rho = 300 \text{ g cm}^{-3}$ . The radius and pulse duration are the values that were found to be optimal in the previous study. We considered mono-energetic and exponential energy distributions  $\exp(-\mathcal{E}/\bar{\mathcal{E}})$ . The code was also run without angular scattering for the monoenergetic beam. The results are given in figure 4. They show that (i) scattering has little effect on the optimal mean energy and increases the ignition energy by 10–20%, (ii) the minimum ignition energy is  $\approx 22 \text{ kJ}$ , (iii) the optimal energy is  $0.75\text{--}1.5 \text{ MeV}$  for a monoenergetic distribution and (iv) the optimal mean energy is  $0.3\text{--}0.5 \text{ MeV}$  for an exponential distribution. (We remark that these results concern homogeneous DT spheres. Realistic density distributions of compressed fuels, with low density plasmas

surrounding the dense core would lead to sensibly higher optimal electron average kinetic energies.)

We have developed a simple model that accurately reproduces these results. First, by running the Monte Carlo routine for densities from  $100$  to  $1000 \text{ g cm}^{-3}$  and temperatures from  $1$  to  $10 \text{ keV}$  we have found that the penetration depth (along the initial electron axis) by which 90% of the energy is deposited is accurately approximated by

$$\mathcal{P}_{90\%}(\mathcal{E}_0) \simeq 0.57 \frac{\mathcal{E}_0^2}{0.66\mathcal{E}_0 + 0.34} \left( \frac{\rho}{300 \text{ g cm}^{-3}} \right)^{0.066} \text{ g cm}^{-2}, \quad (2)$$

and can be fitted by the simpler expression

$$\mathcal{P}_{90\%} \simeq [\mathcal{E}/(1.4 \text{ MeV})][\rho/(300 \text{ g cm}^{-3})]^{0.066} \text{ g cm}^{-2}, \quad (3)$$

for  $1.5 \leq \mathcal{E} \leq 5 \text{ MeV}$ . We then assume that: (i) equation (1) gives the energy that must be deposited up to a depth of  $1.2 \text{ g cm}^{-2}$ , (ii) the penetration depth is approximated by equation (3); (iii) angular scattering increases the ignition energy by a factor of 1.2 and (iv) electron energy deposition is uniform in depth up to  $\mathcal{P}_{90\%}$ . This gives

$$E_{\text{ig}}^{\text{mon}} \simeq 22 \left( \frac{\rho}{300 \text{ g cm}^{-3}} \right)^{-1.85} \max \left( 1, \frac{\mathcal{E}}{1.7 \text{ MeV}} \right) \text{ kJ,} \quad (4)$$

$$E_{\text{ig}}^{\text{exp}} \simeq 22 \left( \frac{\rho}{300 \text{ g cm}^{-3}} \right)^{-1.85} \times [1 - \exp\{-1.54/\bar{\mathcal{E}}(\text{MeV})\}]^{-1} \text{ kJ,} \quad (5)$$

for monoenergetic beams and for beams with exponential energy distributions, respectively. These approximations are also plotted in figure 4, for DT plasmas with a density of  $300 \text{ g cm}^{-3}$ .

We also notice that the curves of figure 4 show the same trends as those computed in a previous study by us on the HiPER targets [8] and in a similar study by the LLE group [29].

The goal of the above study was to determine the dependence of the required electron beam energy on hot electron temperature and spectrum. A model problem was therefore setup. Of course, in an actual case the properties of the electron beam are likely to change in time, since the properties of the interaction region (e.g. the density scale-length) evolve rapidly during ultraintense laser irradiation. Aspects of this issue were studied in [17, 30].

The calculations presented above give the minimum beam energy required on entering the core, and do not consider the transport of the electrons to the core. Further work is required to determine the initial electron beam parameters required for ignition, and eventually the ignition laser requirements. Some aspects of the transport of electrons in the halo surrounding the dense core are discussed in section 4.2.

#### 4.2. Simulations of ignition of a model fuel assembly, including self-generated fields

The study of electron transport in a low density corona requires kinetic (e.g. particle-in-cell) codes and can only be performed for systems much smaller than an actual target. In the halo of the compressed fuel, with density of the order of a few  $\text{g cm}^{-3}$ , the effect of self-generated fields can instead be studied by simulations with hybrid codes, which describe fast electrons

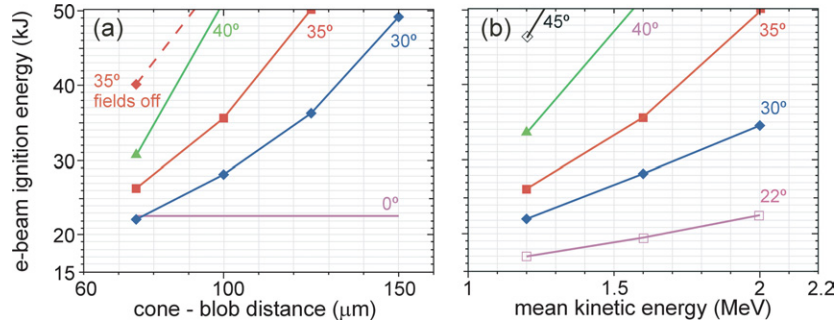


**Figure 5.** (a) Ignition energy as a function of the electron source–core distance for  $\bar{\mathcal{E}} = 1.6$  MeV. Curves are labelled with the mean divergence half-angle. The dashed line corresponds to the case with self-generated fields artificially suppressed. (b) Ignition energies as a function of the mean kinetic energy of the relativistic electron beam with the mean divergence half-angle as parameter for a cone (electron source)–core distance  $d = 100 \mu\text{m}$ .

kinetically and the background plasma by a resistive MHD model. Notice that in cone-inserted fast ignitors one aims at producing the hot electrons just at the tip of the cone, at a small distance from the highly compressed plasma core. We have then studied ignition of a spherical fuel core with a peak density of  $500 \text{ g cm}^{-3}$ , surrounded by a low density halo as a function of injected electron energy, distance  $d$  of cone tip (i.e. the electron source) to dense core, initial divergence half-angle ( $\theta$ ) and mean kinetic energy of the electron beam  $\bar{\mathcal{E}}$ . We have performed integrated simulations including hybrid PIC modelling of fast electron transport, hydrodynamics, DT ignition and  $\alpha$ -particle transport. Electron transport in the cone tip [31] is not considered.

We find that fast electrons propagate up to the dense core and deposit there (by classical Coulomb collisions) a significant fraction of their energy without beam disruption or breaking-up due to the self-generated magnetic fields. The main results are summarized in figure 5, showing the electron beam energy required for ignition versus  $\langle\theta\rangle$ ,  $\bar{\mathcal{E}}$  and  $d$ . Notice the strong dependence of  $E_{\text{ig}}$  on  $\langle\theta\rangle$ ,  $\bar{\mathcal{E}}$  and  $d$ , and the important role played by self-generated fields via beam collimation. Comparison of the ignition energies with that obtained for a perfectly collimated beam ( $\theta = 0^\circ$  and fields turned off) indeed shows that for  $\langle\theta\rangle = 30^\circ$  and  $d = 75 \mu\text{m}$ , the beam is almost perfectly collimated. For higher values, beam collimation is still important, but the beam diverges as it propagates towards the dense core. We found ignition energies 20–30% lower than those reported in previous works [22, 23] due to the sharper radial profile of the fast electron beam assumed here (supergaussian instead of gaussian) which concentrates the energy deposition and enhances magnetic field generation at the beam edge. More details on the calculations are given in [32]. If the distance from the electron source to the dense core is smaller than  $125 \mu\text{m}$ , ignition can be achieved by electron beams with energy about 40 kJ for  $\langle\theta\rangle = 30^\circ$ – $35^\circ$  and  $\bar{\mathcal{E}} \leq 1.6$  MeV.

## 5. SI studies

In SI [11] the energy required to ignite a precompressed target is provided by a properly timed strong shock launched at the end of the coasting phase of the implosion, by means of a final spike in the laser pulse (see figure 6). SI is attractive

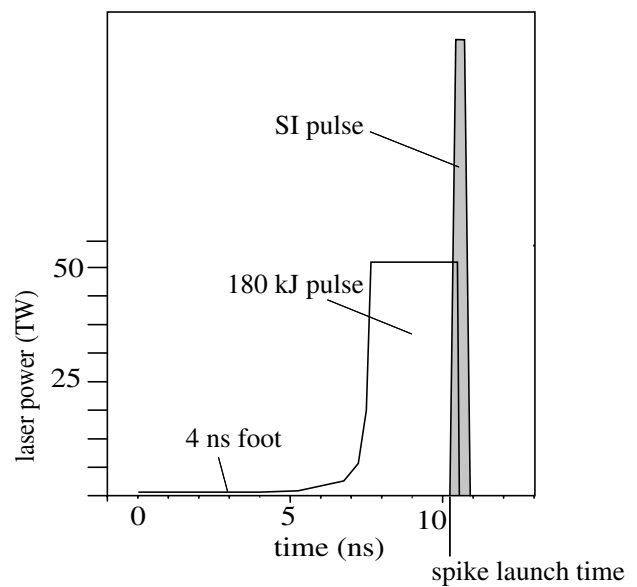


**Figure 6.** Laser pulse for SI. The SI pulse power is not to scale (see main text).

because it does not require any specific ignitor laser nor cone-in-shell targets. Moreover, the physics at work in the hot spot heating is laser driven hydrodynamics, for which calibrated, predictive codes exist. Here, we discuss SI of the HiPER reference capsule. For a detailed presentation, see [33].

### 5.1. Igniting pulse optimization

Two important parameters characterizing the ignition shock are launching time and absorbed laser power. We have studied their optimal values and tolerable variations by means of a series of 1D CHIC [21] simulations. We consider the laser pulse shown in figure 6, which consists of the HiPER compression pulse shown in figure 1(c), followed by an intense spike towards the end of the implosion. The thermonuclear yields calculated by CHIC are plotted in figure 7 as a function of spike launch time and absorbed laser power during the spike. The ignitor pulse is the same for all simulations, with a rise time of 200 ps, a plateau of 300 ps and a 200 ps decrease time. The ignition threshold is found around 50 TW (absorbed power) for a spike launched at 10.1 ns. We define as ‘ignition window’

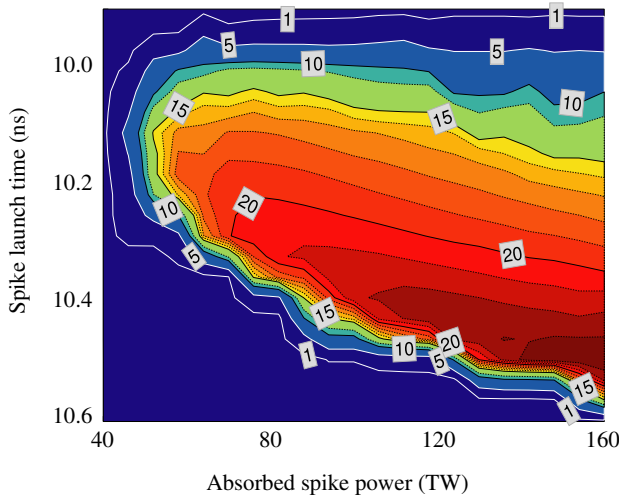


**Figure 7.** Dependence of the target thermonuclear yield in MJ on the launch time and absorbed power of the ignition shocks.

(IW) the time interval ensuring a yield larger than 80% of the maximum yield at given power. One can observe that the IW broadens as (absorbed) power increases from 50 TW up to 80 TW. At 80 TW a 250 ps window warrants a yield larger than 16 MJ. According to figure 7 the ignition window does not significantly widen at powers exceeding 80 TW, and one can anticipate that the laser absorption saturates as will the target gain, hence there is no point in using greater powers. Notice that, for a given spike absorbed power, the dependence of yield on the launch time is not symmetric (in agreement with [11]): a low positive slope in yield appears for early spikes, whereas a steep cliff can be seen for late launch times.

### 5.2. Irradiation scheme

Using the same irradiation pattern as described in section 3.1 for the compression pulse, the 3D ray-tracing package of CHIC predicts an average absorption of 35% during the spike. This means that 230 TW of incident laser power would be necessary for the SI of the HiPER target. Such a low absorption is due to the small value of the critical radius at the shock launching time. Indeed, during the spike, the critical radius varies from 500 to 400  $\mu\text{m}$ , while in order to ensure an optimal irradiation uniformity at the beginning of the target implosion, the focal spots have a gaussian intensity distribution, with a 610  $\mu\text{m}$  radius at  $1/e$ . Therefore, a significant part of the incident laser rays misses the critical surface during the spike laser pulse. A solution is to use dedicated laser beams to deliver this part of the pulse. By decreasing the focal spot diameter and optimizing the radial intensity distribution in the focal spot one may increase the absorption up to 50–60%. We have found that a 160 TW, 80 kJ ignition pulse with 400  $\mu\text{m}$  radius, top-hat focal spot, delivered by specific beam lines ignites the HiPER target. In order to assess the possibility to irradiate the target with a limited number of beamlines, we calculated the ignition of a spherical fuel assembly driven by clusters of ignition beams placed at different polar angles. Preliminary simulations indicate that the thermonuclear yield remains almost constant (20 MJ) whatever the angle is, this being mainly due to a very efficient thermal smoothing in the conduction region.

### 5.3. 2D simulations of shock ignition of a perturbed fuel assembly

Another important issue for shock ignition concerns Rayleigh–Taylor instability (RTI), which may strongly perturb the shell–hot spot interface during the shell deceleration and subsequent stagnation. As a first study of this important problem, we performed 2D simulations of shock ignition of a non-uniformly compressed HiPER baseline target. Compression was driven by a pulse with an  $l = 12$  Legendre perturbation, which resulted in a perturbed compressed core. The perturbations seed RTI at deceleration and stagnation. A 150 TW SI laser spike was then delivered by beams oriented at  $54.7^\circ$  with respect to the polar axis in order to produce a nearly spherical ignitor shock. The simulations show that despite the strong RTI occurring at stagnation, the target ignites and produces 20 MJ of thermonuclear energy, i.e. just the same energy yield as obtained from a perfectly symmetric (1D spherical) simulation performed with the same code. Indeed the simulations indicate that the strong shock mitigates RTI; this is shown, e.g. by the comparison between figure 8(a) (showing density and temperature maps of a compressed target, without the final shock) and figure 8(b) (showing the density maps in the present SI case). This result is in agreement with the improved stability of implosions driven by shock-ignition-like pulses observed in Omega experiments [34], where measurements of areal density and neutron yield indicate a dramatic saturation of the RTI at high convergence ratios (figures 7 and 9 in [34]). The authors invoke a shortening of the RTI stage due to the impulsive acceleration driven by the spike shock wave. According to our observations, two physical mechanisms contribute to the apparent immunity of the shock ignition scheme with regard to RTI: first, the shock transit on the perturbed interface gives birth to a Richtmyer–Meshkov instability that partially reverses the perturbation (clearly apparent in figure 8); the second effect is that a converging shock, though oscillating, is intrinsically stable and will produce anyhow the required pressure when focusing at target centre. Moreover, the comparison of our figure 8 to figure 36 of [35] suggests that fire polishing may also occur in the early deflagrative phase of the combustion.

## 6. Conclusions

The rationale for the choice of the reference target concept for HiPER, and the relevant key physics issues were discussed in previous papers. In this paper we have presented new results, first on the design of a realistic irradiation scheme and its consequences on implosion symmetry. Concerning the ignition stage, we have improved the description of hot electron interaction with the dense core, showing the effect of scattering and also finding a scaling of the ignition energy with the average kinetic energy of the electron beams. This confirms that the *temperature* of the hot electrons should be about 1 MeV. In addition, we have shown that the hot electron source should be as close as possible to the dense fuel core (possibly at a distance below 100  $\mu\text{m}$ ) and should have a modest divergence. However magnetic fields in the halo surrounding the highly compressed fuel can help to limit beam divergence. So far, three crucial issues have not yet been addressed in detail. These concern (i) the effect of short wavelength hydrodynamic

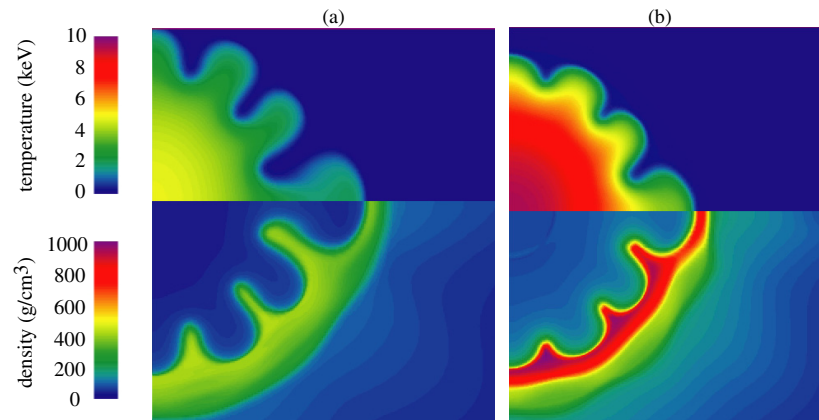


**Figure 8.** CHIC 2D simulations of shock ignition of a perturbed ( $l = 12$ ) target. Electron temperature maps (upper frames) and density (lower frames) maps at ignition time in the no-shock case (a) compared with the shock ignition case (b).

perturbations (seeded by target corrugations and imprint, and amplified by RTI and Richtmyer–Meshkov instability) on target compression; (ii) the (radiation-)hydrodynamics effects of the cone and (iii) generation of the hot electrons and their transport to the dense fuel. The HiPER modelling and target design team plans to address them in the near future.

As an alternative to standard fast ignition, we have also studied shock ignition. We have determined beam requirements to ignite the HiPER reference target, and also studied the effect of low-mode non-uniformities on ignition. A key aspect deserving serious attention concerns the interaction of the intense laser pulse and possible laser–plasma instabilities degrading absorption. Another relevant topic is the interaction of the (presumably not uniform) igniting shock with the compressed fuel, presenting both long and short scale inhomogeneities. We shall study this last issue by very high resolution 2D simulations.

## Acknowledgments

This work was performed in the framework of the HiPER project (EC FP7 project number 211737). Two authors (SA and AS) were supported in part by the Italian Ministry of University and Research projects FIRB RBNE03N48B ‘BLISS’ and PRIN 20072KW45J. JJH was supported by the research projects ENE2006-0336 and CAC07-13.

## References

- [1] Dunne M. 2006 *Nature Phys.* **2** 2
- [2] Dunne M. *et al* 2007 *HiPER—Technical Background and Conceptual Design Report* Rutherford Appleton Laboratory, report RAL-TR-2007-008; [www.hiper-laser.org](http://www.hiper-laser.org)
- [3] Tabak M. *et al* 1994 *Phys. Plasmas* **1** 1626
- [4] Campbell E.M., Freeman R.R. and Tanaka K.A. (guest ed) 2006 Special Issue on Fast Ignition *Fusion Sci. Technol.* **49** 3
- [5] Kodama R. *et al* 2001 *Nature (London)* **412** 798
- [6] Hatchett S.P. *et al* 2006 *Fusion Sci. Technol.* **49** 327
- [7] Atzeni S., Schiavi A. and Bellei C. 2007 *Phys. Plasmas* **14** 052702
- [8] Atzeni S., Schiavi A., Honrubia J.J., Rybeire X., Schurtz G., Nicolai Ph., Olazabal-Loumé M., Bellei C., Evans R.G. and Davies J. R. 2008 *Phys. Plasmas* **15** 056311
- [9] Nagatomo H. *et al* 2007 *Phys. Plasmas* **14** 056303
- [10] Ribeyre X. *et al* 2008 *Plasma Phys. Control. Fusion* **50** 025007
- [11] Betti R. *et al* 2007 *Phys. Rev. Lett.* **98** 155001
- [12] Lindl J.D. 1998 *Inertial Confinement Fusion* (New York: Springer)
- [13] Betti R., Solodov A.A., Delettrez J.A. and Zhou C. 2006 *Phys. Plasmas* **13** 100703
- [14] Anderson K. and Betti R. 2004 *Phys. Plasmas* **11** 5
- [15] Atzeni S. *et al* 2008 *J. Phys.: Conf. Ser.* **112** 022062
- [16] Wilks S.C., Kruer W.L., Tabak M. and Langdon A.B. 1992 *Phys. Rev. Lett.* **69** 1383
- [17] Chrishman B. *et al* 2008 *Phys. Plasmas* **15** 056309
- [18] Xiao J. and Lu B. 1998 *J. Opt.* **29** 282
- [19] Hallo L. *et al* 2009 *Plasma Phys. Control. Fusion* **51** 014001
- [20] Betti R. *et al* 1998 *Phys. Plasmas* **5** 1446
- [21] Maire P.-H. *et al* 2007 *SIAM J. Sci. Comput.* **29** 1781
- [22] Honrubia J.J. and Meyer-ter-Vehn J. 2006 *Nucl. Fusion* **46** L25
- [23] Honrubia J.J. and Meyer-ter-Vehn J. 2008 *Journal of Phys.: Conf. Ser.* **112** 022055
- [24] Atzeni S. 1999 *Phys. Plasmas* **6** 3316
- [25] S. Atzeni *et al*. 2005 *Comput. Phys. Commun.* **169** 153
- [26] Atzeni S. and Tabak M. 2005 *Plasma Phys. Control. Fusion* **47** B769
- [27] Atzeni S., Schiavi S. and Davies J.R. 2009 *Plasma Phys. Control. Fusion* **51** 015016
- [28] Solodov A.A. and Betti R. 2008 *Phys. Plasmas* **15** 042707
- [29] Solodov A.A., Betti R., Delettrez J.A. and Zhou C.D. 2007 *Phys. Plasmas* **14** 062701
- [30] Sagakami H., Johzaki T., Nagatomo H., Nakamura T. and Mima K. 2008 *J. Phys.: Conf. Ser.* **112** 022070
- [31] Johzaki T., Sentoku Y., Nagatomo H., Sakagami H., Nakao Y. and Mima K. 2009 *Plasma Phys. Control. Fusion* **51** 014002
- [32] Honrubia J.J. and Meyer-ter-Vehn J. 2009 *Plasma Phys. Control. Fusion* **51** 014008
- [33] Ribeyre X. *et al* 2009 *Plasma Phys. Control. Fusion* **51** 015013
- [34] Theobald W. *et al* 2008 *Phys. Plasmas* **15** 055503
- [35] Nakai S. and Takabe H. 1996 *Rep. Prog. Phys.* **59** 1071